

Communication sheets using printed organic nonvolatile memories

Tsuyoshi Sekitani¹, Yoshiaki Noguchi¹, Shintaro Nakano¹, Koichiro Zaito¹, Yusaku Kato¹,
Makoto Takamiya², Takayasu Sakurai³, and Takao Someya^{1*}

¹ Quantum-Phase Electronics Center, School of Engineering, The University of Tokyo, Tokyo 113-8656, Japan

² VDEC, The University of Tokyo, Tokyo 153-8904, Japan

³ Center for Collaborative Research, The University of Tokyo, Tokyo 153-8904, Japan

Abstracts

Human-scale communication sheets have been manufactured using printing processes with integrating an organic nonvolatile FeRAM with nondestructive read capability and plastic MEMS switches. The communication route is dynamically formed by MEMS switches and stored by the memory. The “1”-“0” ratio of the memory exceeds 10^3 after 10^4 cycles in air.

1. Introduction:

Ambient electronics is expected to open up a new continent of applications. This paper reports a communication sheet which can build infrastructure for the ambient electronics together with the wireless power transmission sheet previously published in IEDM [1,2]. Combining relatively long-distance wired communication and mm-scale wireless communication, the sheet offers a new communication method that enables multiple electronic objects scattered over the sheet to communicate contactlessly with each other by establishing communication paths easily without cumbersome physical connections (Fig. 1). Since the information transmitted over

the sheet is confined in small space close to ad hoc routed paths, the system provides more secure communication against tapping compared with ordinary wireless LAN and is free from issues related with radio frequency band allocation which has been already tight.

The communication route is dynamically formed using printed plastic MEMS switches. In order to store the routing information, a nonvolatile memory cell array based on printing processes is developed, which is ferroelectric random access memory (FeRAM) [3]. Each cell consists of one organic ferroelectric memory transistor and two organic transistors (Fig. 2). Although all previously reported organic nonvolatile memory cells utilized a one-transistor (1T) structure [4,5], this is the first demonstration of a nonvolatile, nondestructive memory using a three-transistor (3T) structure, which maintains a time-continuous current and/or voltage. This feature is well suited for programming actuators such as MEMS switches distributed over large area. Moreover, the 3T structure nonvolatile memory cells can significantly reduce the chance of a false writing, compared with 1T structure cells.

The effective communication area is $21 \times 21 \text{ cm}^2$. The sheet contains a two-dimensional array of 8×8 communication cells. The “1”-“0” current ratio of organic

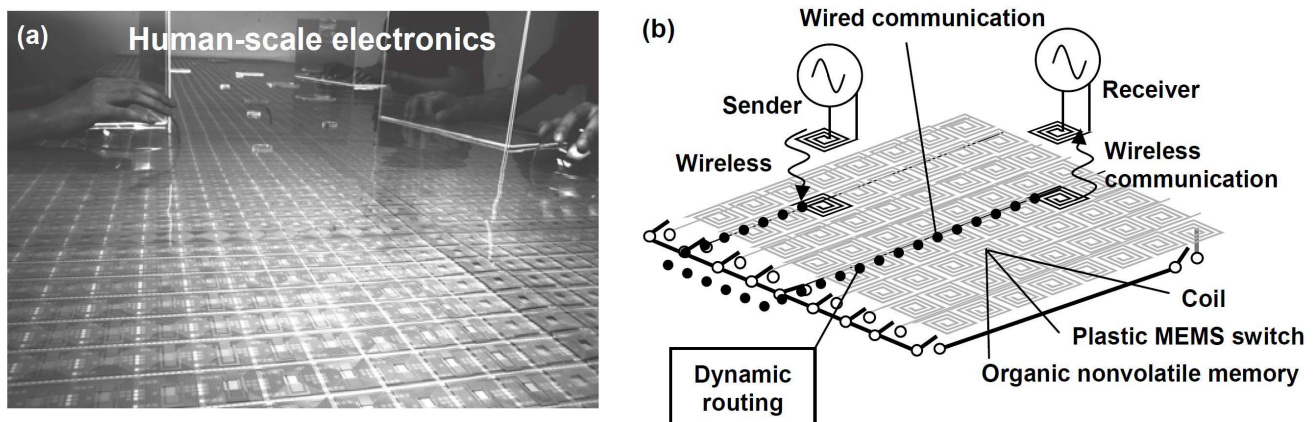


Fig. 1: Communication sheet. (a) An image of the manufactured large-area communication sheet. The whole surface of the table is covered with multiple prototype communication sheets. (b) A principle of the communication sheet.

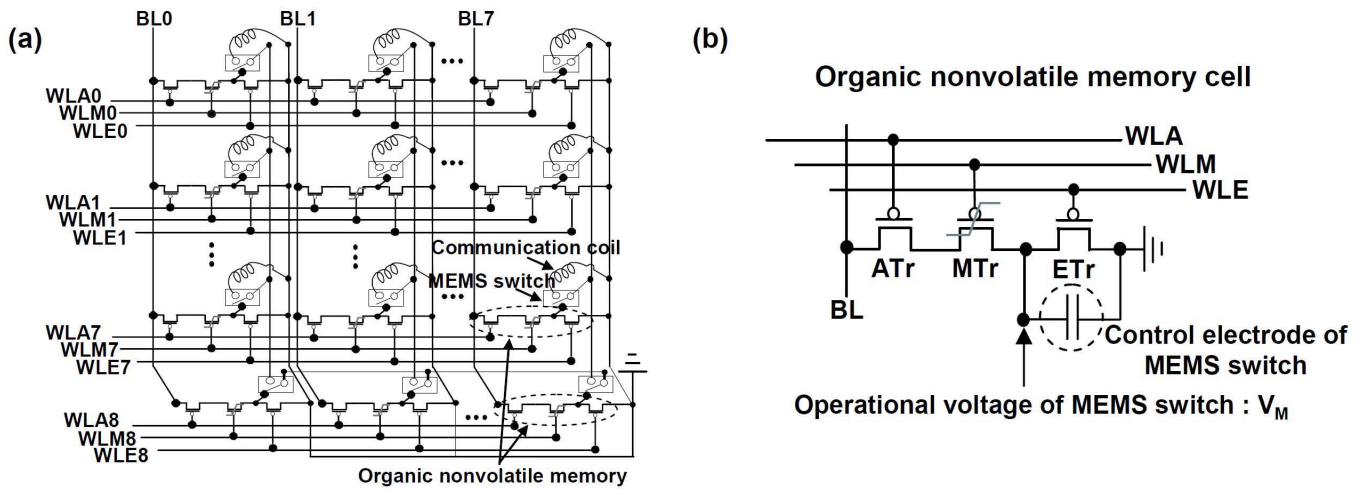


Fig. 2: Circuit diagram. (a) This communication sheet comprises communication coils, MEMS switches, and organic nonvolatile memories. The periodicity is 25.4 mm. (b) Each memory cell comprises an access transistor (ATr), a memory transistor (MTr), and an erase transistor (ETr).

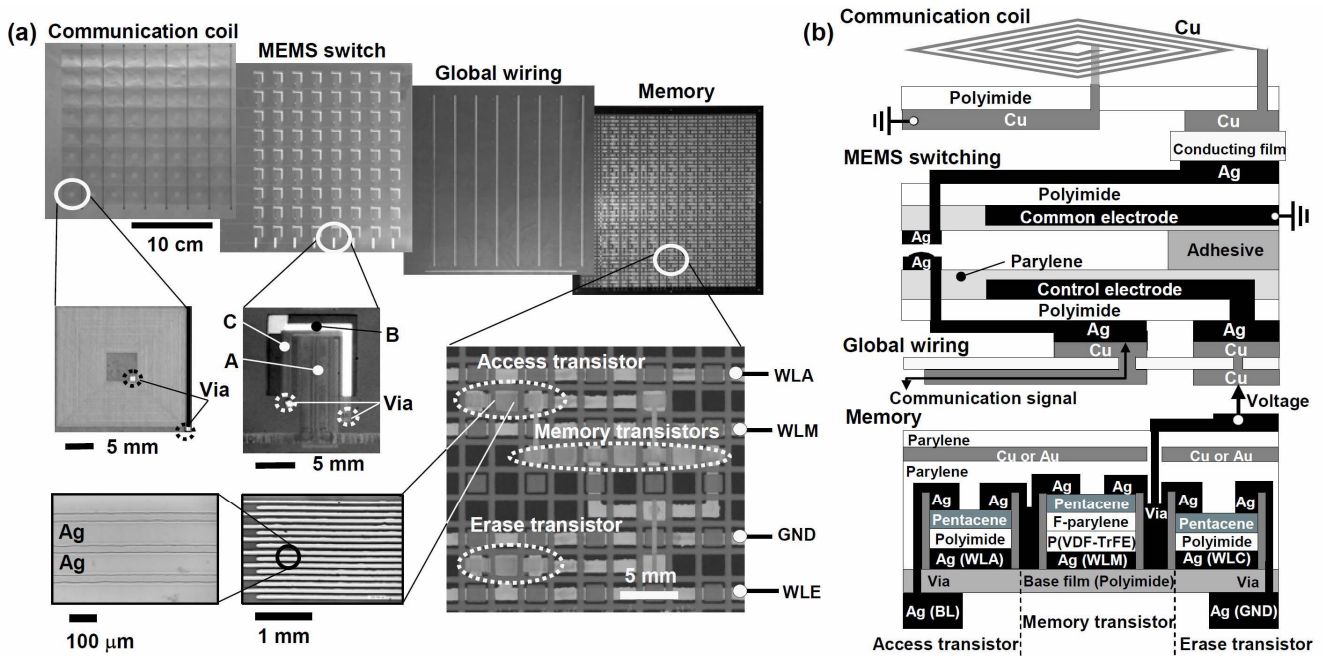


Fig. 3: Communication sheet comprising communication coils, MEMS switches, global wiring, and organic nonvolatile memories. (a) Device assembly. **Coil:** The inductance and resistance of the coil are 27 μH and 25 Ω , respectively. **MEMS:** (A) Electrodes for electrostatic attraction as the common and control electrodes of the MEMS switches. (B) and (C) Electrodes for the transmission of the communication signal. **Memory:** (b) A cross-sectional illustration. A circuit diagram in Fig. 2 (b).

nonvolatile memory exceeds 10^5 . The retention time is more than 15 days in air.

The thickness and weight of the entire sheet are 1 mm and 100 g, respectively.

2. Device manufacturing process:

Each cell of the organic nonvolatile memory array (Fig. 3) comprises three organic transistors; an access transistor, a memory transistor, and an erase transistor. All the metal wires and electrodes are patterned by inkjet using silver nanoparticles. Polyimide is inkjetted to form gate dielectric layers for access and erase transistors, while

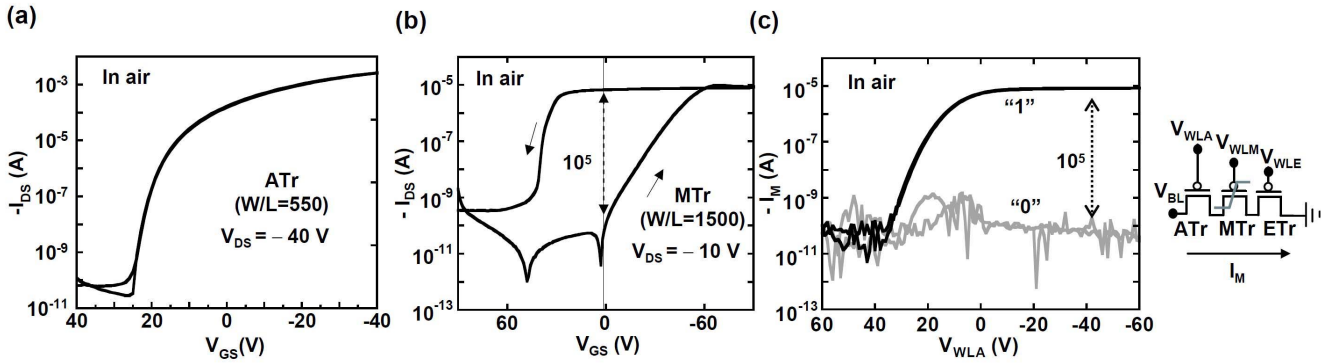


Fig. 4: Organic nonvolatile memory. Transistor characteristics of stand-alone (a) ATr and (b) MTr. (c) Transfer characteristics of the memory cell with a 3T structure. The “1” state is attained after applying voltages of $V_{WLA} = V_{WLE} = -40$ V, $V_{BL} = +40$ V, and $V_{WLM} = -60$ V, while the “0” state is attained after applying voltages of $V_{WLA} = V_{WLE} = -40$ V, $V_{BL} = -40$ V, and $V_{WLM} = +60$ V. Read-out is performed by applying $V_{WLA} = +60$ V to -60 V, $V_{WLE} = -40$ V, and $V_{BL} = -10$ V, while $V_{WLM} = 0$ V. All the measurements are performed in air. A 3T memory cell exhibits a large “1”-“0” current ratio exceeding 10^5 in air.

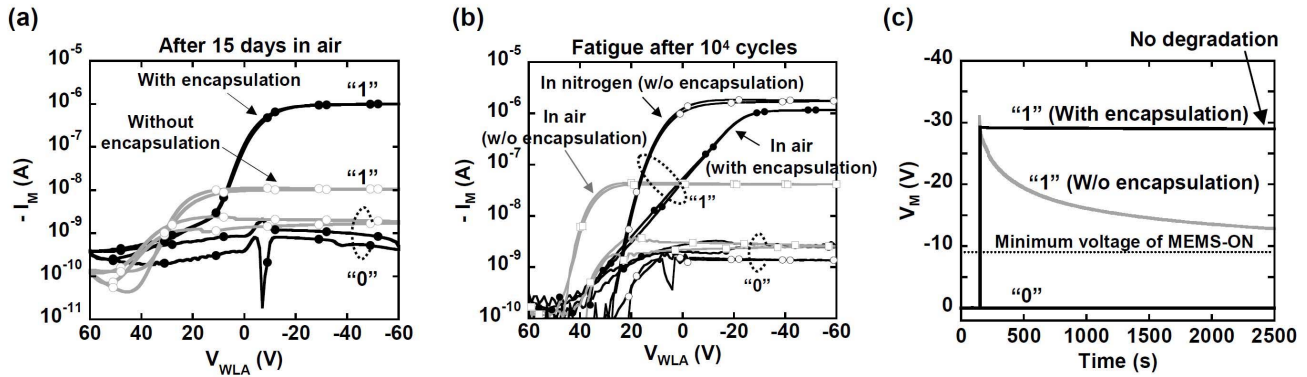


Fig. 5: Memory characteristics and plastic MEMS switch driven by an organic memory. (a) Retention characteristics in air: Transfer curves of the memory cell after storage in air for 15 days. (b) Fatigue characteristics in air and a nitrogen environment: Transfer curves after 10^4 writing and erasing cycles. (c) Plastic MEMS switch driven by an organic memory. Voltages (V_M) through an organic memory cell when the memory is “1” or “0” in air. Measurements are performed at the voltages of $V_{WLA} = -40$ V and $V_{BL} = -40$ V, while $V_{WLM} = V_{WLE} = 0$ V. When 9 V are applied to the control electrode of the MEMS switch, the resistance decreases to 23Ω .

poly(vinylidene fluoride/trifluoroethylene) [P(VDF/TrFE)] [6] is used to form a ferroelectric gate dielectric layer for memory transistors. The surface of P(VDF-TrFE) is coated with fluoride parylene. Pentacene channel layers deposited in a vacuum and source/drain electrodes are directly formed by inkjet to build the top contact devices.

All the transistors are coated with organic/metallic encapsulation layers and annealed for a threshold control. The channel length is $30 \mu\text{m}$ for all the transistors, while the width of the access, memory, and erase transistors are $16.5 \mu\text{m}$, $45 \mu\text{m}$, and $300 \mu\text{m}$, respectively.

The MEMS switch is formed by using inkjet printing and NC mechanical punching system [1]. The electrodes

for communication and those for control and common are patterned on a $25\text{-}\mu\text{m}$ -thick polyimide membrane.

The global wiring sheet comprises 9 copper lines with the thickness of $18 \mu\text{m}$ for interconnection between MEMS switches. The resistance is less than 1Ω .

The communication coil comprises square copper coils with an outer diameter of $25 \mu\text{m}$. Both the width and spacing of the copper lines are $100 \mu\text{m}$. The number of turns is 53. The inductance and resistance are $27 \mu\text{H}$ and 25Ω , respectively.

The assembly (Fig. 3): A plastic MEMS switch array laminated together with the communication coil sheet and

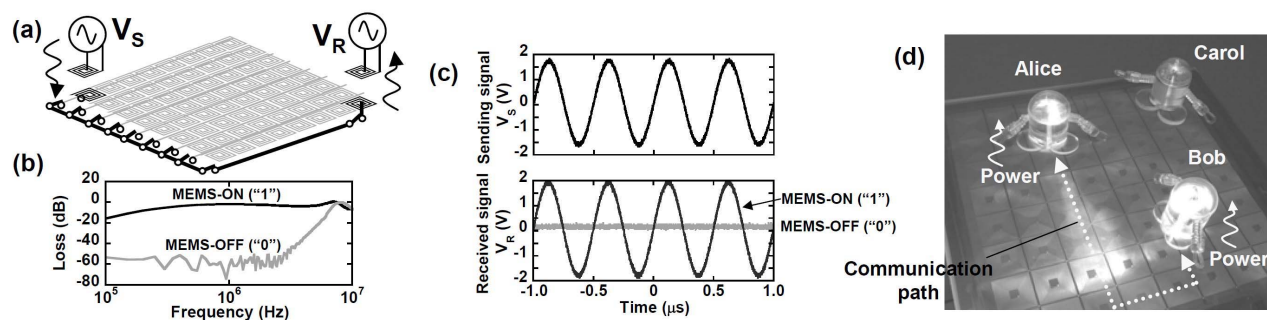


Fig. 6: Communication. (a) Schematic illustration of the communication system. (b) Transmission loss from “ V_S ” to “ V_R ” as a function of frequency. (c) When a signal of V_S is applied from the “sender” end, a signal of V_R is observed at the “receiver” end when the MEMS switch is ON (“1”). The frequency is 2 MHz. The received signal is less than 1 mV when the MEMS switch is OFF (“0”). (d) The communication sheet works cooperatively with the wireless power transmission sheet. The power sheet under the communication sheet can transmit power to two robots with LEDs wirelessly.

the global wiring sheet comprising copper lines for the interconnections between the MEMS switches.

3. Device characteristics:

The pentacene transistors for access and erase transistors exhibit mobility of $1 \text{ cm}^2/\text{Vs}$ and an on/off ratio of 10^5 . A memory transistor exhibits large hysteresis at $V_{GS} = 0 \text{ V}$.

The memory with a 3T structure (Figs. 4 and 5): A 3T memory cell exhibits a large “1”-“0” current ratio of 10^5 in air. The current ratio exceeds 10^3 after it is stored in air for 15 days owing to the organic/metallic hybrid encapsulation [7]. Furthermore, the memory retains a high ratio of above 10^3 after 10^4 write cycles in air. The time for “0” to “1” is 40 ms, while the time for “1” to “0” is 10 ms. With the decrease in the thickness of P(VDF-TrFE), the writing/erasing voltages decrease to 20 V.

A plastic MEMS switch (Fig. 5 (c)) is driven by an organic nonvolatile memory cell. An organic memory cell can supply stable voltages above 10 V to the control electrode of the MEMS switch when the memory is in write-state. When 9 V is applied to the control electrodes, the resistance changes from $>10^6 \Omega$ to 20Ω . Maximum frequency response of the MEMS switch is 1 KHz.

The communication (Fig. 6): An organic memory cell can supply continuously stable voltages of above 10 V to the control electrode of the MEMS switch when the memory is in the “1”. The communication signal is transmitted at 2 MHz, which is the resonance frequency of the system. The on/off ratio of the MEMS switch in the communication signal exceeds 10^3 . The communication sheet can cooperatively work with the power transmission sheet.

Acknowledgment: This study was partially supported by Special Coordination Funds for Promoting and Technology, the Ministry of Education, Culture, Sports, Science and Technology and JST/CREST. We also thank Toray Engineering Co., Ltd. for providing high-performance P(VDF-TrFE), Kyocera Chemical Cooperation for a high-purity polyimide precursors (KEMITITE CT4112), and Daisankasei Co., Ltd. for a high-purity parylene (diX-SR).

References:

- [1] T. Sekitani, M. Takamiya, Y. Noguchi, S. Nakano, Y. Kato, K. Hizu, H. Kawaguchi, T. Sakurai, and T. Someya, 2006 IEDM 11.1.
- [2] T. Sekitani, M. Takamiya, Y. Noguchi, S. Nakano, Y. Kato, T. Sakurai, and T. Someya, Nat. Mater. 6, 413 (2007).
- [3] H. Ishiwara, M. Okuyama, and Y. Arimoto, Ferroelectric Random Access Memories – Fundamentals and Applications, (Springer-Verlag, Berlin 2004).
- [4] R. C. Namer, C. Tanase, P. W. M. Blom, G. H. Gelinck, A. W. Marsman, F. J. Touwslager, S. Setayesh, and D. M. De Leeuw, Nat. Mater. 4, 243 (2005).
- [5] M. Musherush, A. Facchetti, M. Lefenfeld, H. E. Katz, and T. J. Marks, J. Am. Chem. Soc. 125, 9414 (2003).
- [6] T. Furukawa, Phase Transitions 18, 143 (1989).
- [7] T. Sekitani and T. Someya, Jpn. J. Appl. Phys. 46, 4300 (2007).